JOURNAL OF MATERIALS SCIENCE 23 (1988) 643–648

Slow fracture in a homopolymer and copolymer of polyethylene

XICI LU*, XUQING WANG*, NORMAN BROWN
Department of Materials Science and Engineering, University of Pennsylvania, Philadelphia, Pennsylvania 19104, USA

The slow crack-growth behaviours of a high-density polyethylene and an ethylene–hexene copolymer with 4.5 butyl chains per 1000 carbon atoms are compared. The slow crack-growth rate in the copolymer is about 10^2 to 10^3 times slower than for the homopolymer. The two polymers are compared with respect to their kinetics of slow crack growth, the morphology of the damage zone that grows from a notch, the stress–strain behaviour and the temperature dependence of the rate of damage. The results suggest that the major effect of the butyl branches is to decrease the rate of disentanglement which governs the process of slow crack growth.

1. Introduction

Polyethylene exhibits a slow time-dependent fracture at low stresses in the vicinity of room temperature. We will call this phenomenon "low stress brittle fracture" (LSBF). A high-density homopolymer fails about 10^2 to 10^3 times faster than an ethylene–hexene copolymer of comparable molecular weight. The copolymer has 4.5 butyl branches per 1000 carbon atoms. Thus, the homopolymer is used for milk bottles and the copolymer is used in a critical application such as piping for natural gas. Why 4.5 butyl branches per 1000 carbons should make such a large difference in LSBF is not well understood.

In this paper these two polyethylenes will be compared with respect to their kinetics, the microstructural changes that occur during LSBF, and other properties that may be relevant. The process of LSBF will be described in its entirety, starting with the initial damage zone that emanates from a defect to the final stage of complete fracture. Only plane strain conditions will be considered because plane strain usually corresponds to the condition under which polyethylene is used for engineering applications.

The two mechanisms that govern LSBF are the rate of conversion from the elastic to the damaged state (yielding) and the rate of fibril disentanglement which causes fracture. The rate of yielding plays a more prominent role in the homopolymer and the rate of disentanglement is most important in the copolymer. The basis for this conjecture is that a molecule with short branches should be more difficult to pull through a crystalline region than a smoother molecule, and because the homopolymer has a higher yield point than the copolymer. However, why only 4.5 butyl branches per 1000 carbon atoms has such a large effect is still the central question.

The homopolymer has been extensively investigated by Bhattacharya and Brown [1–3] and Lu and Brown [4, 5]. The essential results of these investigations will be presented along with new results on the copolymer. Chan and Williams [6] have also measured slow crack growth in a homopolymer and a copolymer of polyethylene. Bubeck and Baker [7] found that increasing the branch length from methyl to hexyl increased the resistance to environmental stress cracking.

2. Experimental procedure

The homopolymer will be called HPE and the ethylene–hexene copolymer, CPE. Both commercial resins are made by Phillips Petroleum under the trade names of Marlex 6006 and TR418, respectively. For HPE, $M_n = 19\,600$, $M_w = 130\,000$ and density = $0.964\,g\,cm^{-3}$; for CPE, $M_n = 15\,000$, $M_w = 170\,000$ and density = $0.945\,g\,cm^{-3}$. The CPE has 4.5 ± 0.5 butyl branches per 1000 carbon atoms. Other branches appear to be negligible in both polymers. Both polymers were compression-moulded in a closed die at 180° C for 10 min and very slowly cooled to room temperature under a pressure of 1.7 MPa.

The previous work on HPE was done mostly with single-edge notched (SEN) tensile specimens (Fig. 1a) 4 mm thick and 18 mm wide with notches ranging from about 0.15 to 0.40 mm deep. The depth of the notches were in the thickness direction in order to obtain plane strain conditions. The CPE specimens (Fig. 1b) were 10 mm thick and 25 mm wide with the primary notch 3.5 mm deep in the thickness direction and contained side notches 1 mm deep as shown in Fig. 1, in order to enhance the plane strain fracture.

The specimens were loaded under a constant stress and the temperature was controlled within ± 0.5° C. The growth of the damage zone was observed with a microscope by measuring the opening of the notch at the following positions (see Fig. 2): (i) the surface of the specimen (AA), (ii) the bottom of the notch as defined by the razor blade (CC), and (iii) the thickness

*Visiting Scientists from the University of Science and Technology of China, Hefei, Anhui, People's Republic of China.

0022–2461/88 $03.00 + .12

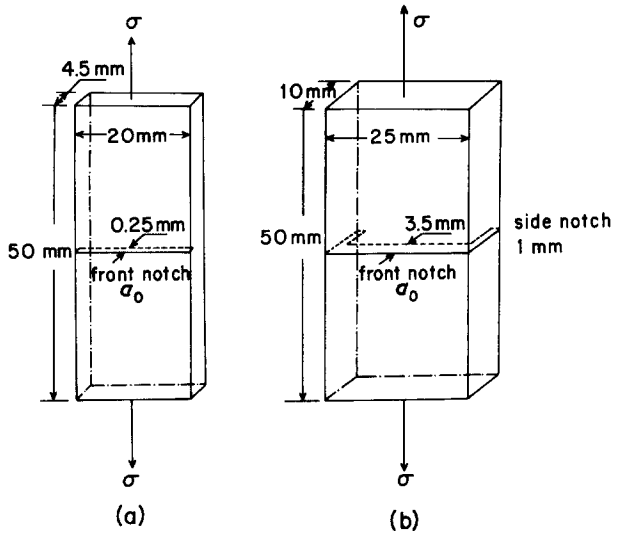

Figure 1 Specimen geometry for (a) HPE, (b) CPE.

of the fibrillar region (BB) as a function of time. For HPE, there was no blunting of the notch so that (CC) and (BB) coincided. Fig. 2 also shows the fibrillar regions for the HPE and CPE as observed during a measurement.

The length of the damage zone and its microstructure were observed after a test by slicing the specimen to a thickness of about 2 mm. The notch in a slice was then opened in a jig to the amount it was open during the test and then was observed in the SEM.

3. Results

Both materials qualitatively exhibit the same three stages of damage. Instantly upon loading there is a deformation zone whose dimensions are appropriately given by the Dugdale theory, namely the length of the damage zone Δa is given by

$$\Delta a = \frac{\pi}{8}\frac{K^2}{\sigma_y^2} \tag{1}$$

and its width at the root of the notch, δ, is for plane strain given by

$$\delta = \frac{K^2}{\sigma_y E(1 - \nu^2)} \tag{2}$$

where K is the stress intensity, σ_y is the yield point, E is Young's modulus and ν is Poisson's ratio.

The fibrillated structure thickens during the next stage until fibril fracture occurs. In the last stage there is a marked acceleration in the velocity of the damage zone, since the initial notch is continually increased as the fibrils continue to fracture and the fibrillar region grows in length.

Representative SEM microstructures of HPE are shown in Fig. 3 during the three stages. The boundary of the damage zone forms practically a straight-line extension of the notch surface, and the angle of the damage zone remains nearly constant at about 10° even during some of the acceleration stage. Figs 3a, b and c are produced by stresses less than one-half the yield point. Figs 3d and e show how the structure changes with increasing stress where the damage zone spreads out and becomes less triangular.

Representative microstructures of CPE are shown in Fig. 4. The shape of the boundary of the damage zone is not straight as for HPE at low stresses. The bottom of the notch is often blunted depending on the

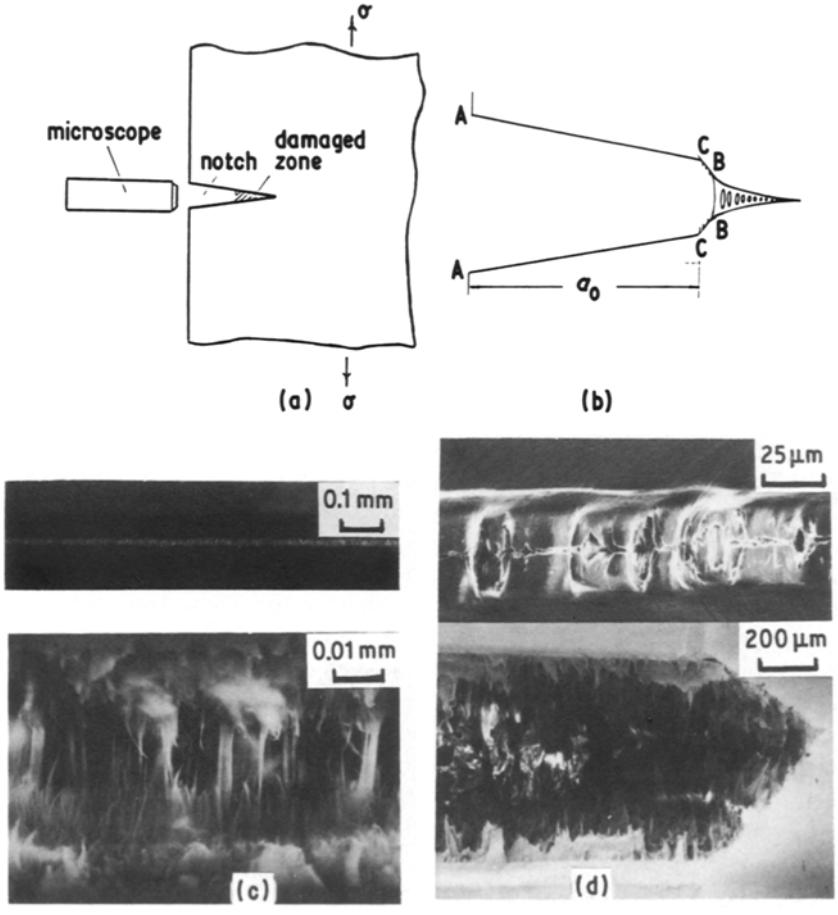

Figure 2 (a) Method of measuring the notch opening; (b) profile of damaged zone in CPE; (c) view into damage zone of HPE; (d) view into damage zone of CPE.

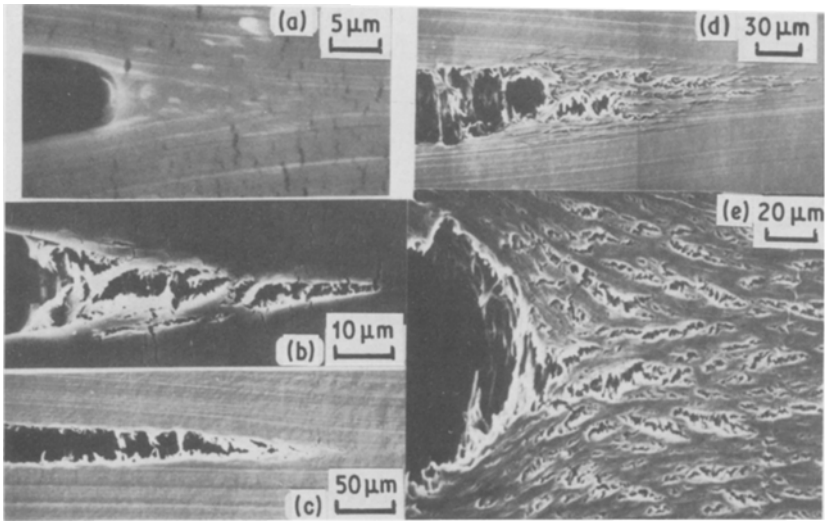

Figure 3 Typical SEM micrographs of HPE. (a) 7.1 MPa, 30° C, 20 min; (b) 12 MPa, 30° C, 10 min; (c) 10 MPa, 30° C, 120 min; (d) 12 MPa, 42° C, 367 min; (e) 15 MPa, 30° C, 84 min. In (a) and (b) the small vertical cracks are artifacts.

stress level. The difference between (CC) and (BB) in Fig. 2 increases with stress. The fibrils in CPE do not fracture as readily as those in the HPE.

Fig. 5 shows the kinetics of damage for HPE where the crack opening displacement at the surface of the specimen and at the bottom of the notch are plotted against time. In addition, the overall creep rate of the specimen is observed. The rate of notch opening displacement, $\dot{\delta}$, is constant for a period after loading and then begins to accelerate when fibril fracture occurs. Prior to well-defined crack growth, the damage zone increases in size by maintaining a shape with a constant angle. When the angle of the deformation is constant, the rates of notch opening as measured at the surface of the specimen and at the bottom of the notch are equal as shown by Fig. 5. For stress less than one-half the yield point, the creep strain in the matrix remains less than the strain for yielding ($\approx 10\%$).

Fig. 6 shows notch opening displacement at the bottom of the notch against time for HPE at various stresses. Curves have been obtained for various notch depths and temperatures. It has been shown that the shape of all these curves and the time to failure, t_f, can be predicted from the initial slope $\dot{\delta}_0$ where

$$t_f = \frac{\alpha a_0 + \delta_c}{\dot{\delta}_0} \tag{3}$$

and α is the angle of the damage zone, a_0 is the initial notch depth and δ_c is a critical displacement which is 0 or 20 μm for the three-point bending and SEN specimens, respectively. Both α and δ_c increase slightly with stress. $\dot{\delta}_0$ is the key parameter which governs LSBF in HPE.

From data such as in Fig. 6, for both three-point bending and SEN specimens it was determined that for HPE

$$\dot{\delta}_0 = C\sigma^m a_0^n e^{-Q/RT} \tag{4}$$

where σ is the stress and Q the activation energy; $m = 5.0$, $n_0 = 1.8$ to 2.0, and Q is 100 to 115 kJ mol^{-1}. C depends primarily on structure in that it varies with density and molecular weight. It is interesting to note that C increases with decreasing density and with decreasing molecular weight [8, 9].

Equation 4 is for a stress less than about one-half of the yield point. At higher stress the specimens fail by a ductile mode which involves large-scale yielding [10].

Fig. 7 shows a typical curve for the kinetics of damage in CPE. The experiments with CPE are generally at higher temperatures than for HPE because the damage rate is about 10^2 to 10^3 times slower for CPE at 80° C when compared to HPE at lower temperatures. Whereas times for complete failure of HPE may range from 10^1 to 10^3 min depending on stress, temperature and notch depth, the failure times for CPE range from 10^3 to 10^6 min. The general shape of the curves is the same in that there is (i) an initial damage zone

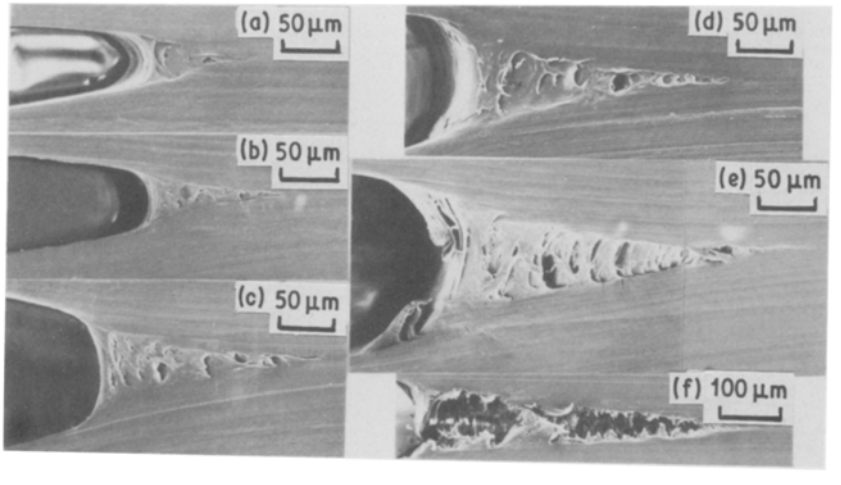

Figure 4 Change in damage zone in CPE with time at $\sigma = 2.55$ MPa, $T = 80°$ C, $a_0 = 2$ mm. (a) 1 min; (b) 10 min; (c) 1230 min; (d) 11 850 min; (e, f) 118 000 min. (e) and (f) are from same specimen but at different cross-sections.

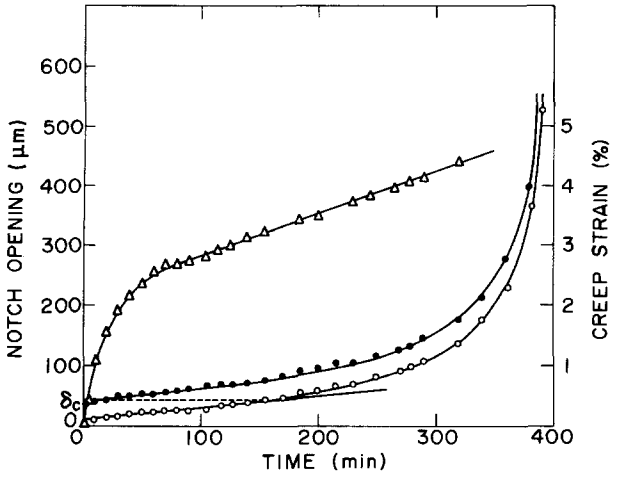

Figure 5 (△) Creep strain in matrix, (●) notch opening at surface (AA), (○) notch opening at tip (CC); all against time for HPE. $a_0 = 0.246$ mm, $\sigma = 10$ MPa, $T = 30°$C.

immediately upon loading, (ii) a period of fibril extension in the damage zone, and (iii) the period of true crack growth during which fibril fracture occurs. The biggest difference between the kinetics of HPE and CPE is the time required to initiate the fracture of the fibrils. The micrographs and the kinetics indicate that the fibrils are much stronger in CPE and the disentanglement rate is slower than for HPE. In Fig. 7 the beginning of fibril fracture occurs when the curves begin to accelerate.

Figs 8 and 9 show the opening of the damage zone against time for CPE at various stresses and temperatures. It is generally observed that the time for initiation of fibril fracture is approximately one-half the time for complete failure, where fibril fracture begins when the curves accelerate.

From the curves at various temperatures, it was determined that the time to failure and the minimum

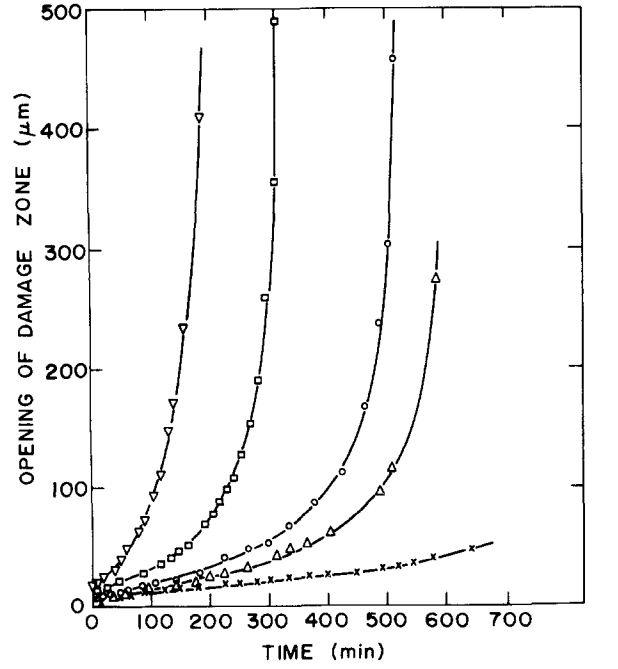

Figure 6 Notch opening at tip against time for HPE at various stresses and a_0 nearly constant. (x) 8 MPa, $a_0 = 0.228$ mm; (△) 9 MPa, $a_0 = 0.253$ mm; (○) 10 MPa, $a_0 = 0.242$ mm; (□) 11 MPa, $a_0 = 0.246$ mm; (▽) 12 MPa, $a_0 = 0.241$ mm.

value of $\dot{\delta}$ prior to fibril fractures give an activation energy of about 130 kJ mol.$^{-1}$

The time to failure against initial stress intensity is shown in Fig. 10. The region of low slope and high stress corresponds to ductile failure. The transition from ductile to brittle failure shows an overshoot. This overshoot is produced by blunting of the initial notch during the initial loading of the specimen. The blunting reduces the stress concentration so that there is a narrow range of stress where the time to failure decreases as the stress decreases. In the brittle failure regime below the knee, the time to failure varies with stress intensity in accordance with K_0^4.

4. Discussion

In order that the damage zone grows, two processes must take place: (i) the fibrils must become weaker with time, and (ii) the damage zone enlarges by transforming material from the elastically deformed state to the fibrillated state. The former process involves the disentanglement of the molecules and the latter process involves yielding.

The stress–strain curves of the two polymers in Fig. 11 give an indication of the comparative importance of these two processes. Since the yield point of HPE is greater than for CPE, it is expected that the nucleation of the fibrils would be easier in CPE. Since the oriented state of the CPE work-hardens and has a much higher strength than for HPE, it is expected that fibril fracture would be more difficult in CPE than in HPE. Since LSBF is of the order of 10^3 times slower in CPE than in HPE, it is concluded that the rate of disentanglement, not yielding, is the dominant mechanism in CPE. The model of highly oriented HPE by Gibson *et al.* [11] is useful for discussing the disentanglement process. Fig. 12a is their model and Fig. 12b is our modification of their model for CPE. Upon crystallization from the melt, it is most likely that the butyl branches will be in the amorphous region, but after orientation their location is more uncertain.

At the temperatures and slow rate at which disentanglement occurs, it is expected that practically no chain scission occurs during the process. Since the amorphous region is above the glass transition temperature, it is expected that the rate-determining process is the sliding of molecular chains through the crystalline regions of the fibrils. From this viewpoint, it is easy to speculate why 4.5 butyl chains per 1000 carbon atoms increases the difficulty of sliding the molecule through the crystal. It seems obvious that pulling a molecule with a butyl chain through a crystal should be more difficult than pulling through the relatively smooth chain of HPE.

Much empirical research by the resin producers has gone into determining the density of branches which will give the lowest rate of slow crack growth. A simple explanation is now given of why there is an optimum density. If there are too few branches then much of the molecule's length will not have its motion impeded by a branch as the molecule moves through the crystal. If there are too many branches, then the overall crystallinity is reduced and the thickness of the

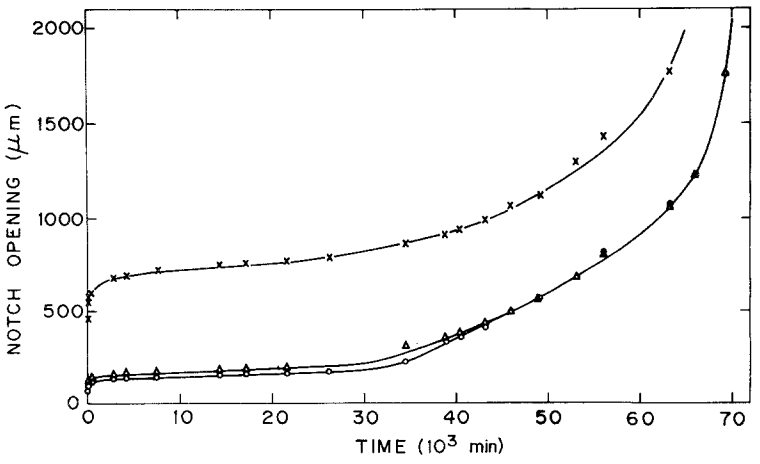

Figure 7 Notch opening against time for CPE. a_0 = 3.5 mm, σ = 2.4 MPa, T = 75° C; (x) AA, (○) BB, (△) CC (see Fig. 2b).

Figure 8 Notch opening at damage zone (BB) against time for CPE at various stresses: (▲) 1.8 MPa, (○) 2.0 MPa, (●) 2.2 MPa, (x) 2.4 MPa, (△) 2.6 MPa, (□) 2.8 MPa. a_0 = 3.5 mm, T = 80° C.

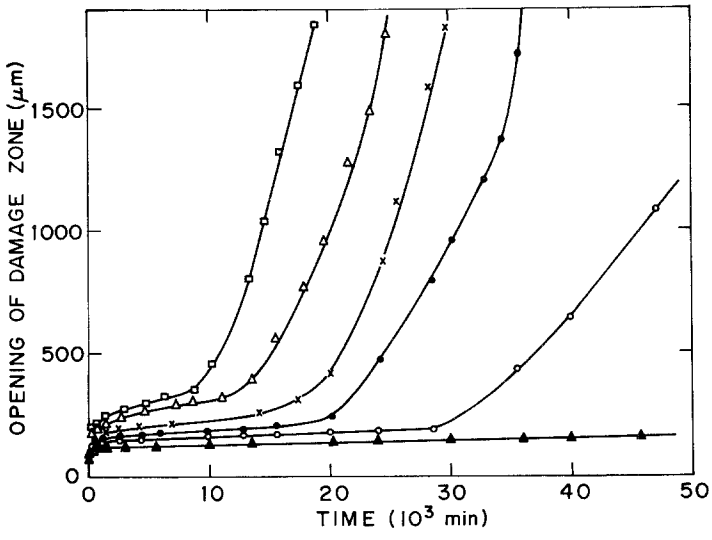

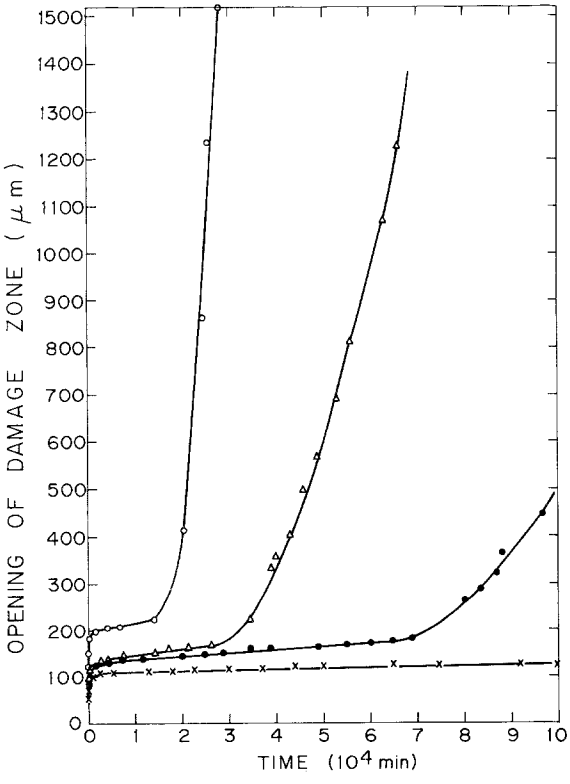

Figure 9 Same as Fig. 8 at various temperatures: (x) 60° C, (●) 70° C, (△) 75° C, (○) 80° C. a_0 = 3.5 mm, σ = 2.4 MPa.

crystalline region is reduced and the resistance to the sliding is reduced. The optimum resistance to sliding is expected when the thickness of the crystal matches the distance between branches. 4.5 branches per 1000 carbons corresponds to 25 nm between branches, which also corresponds to the thickness of lamellar crystals. Data are not yet available that shows the dependence of branch density on the rate of LSBF. The other important factor that determines the rate of disentanglement is the molecular weight [9]. The longer the molecule, the more likely it is that it will act as a tie molecule and pass through more than one crystalline region. The greater the extent of crystal through

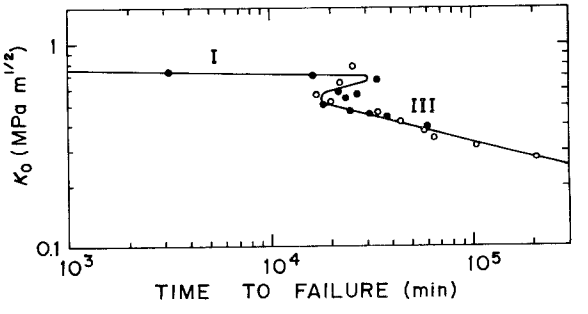

Figure 10 Stress intensity against time to failure for CPE at 80° C. (○) σ = 3.2 MPa, a_0 varied; (●) a_0 = 3.5 mm, σ varied. For Region III (1/slope) = −4.

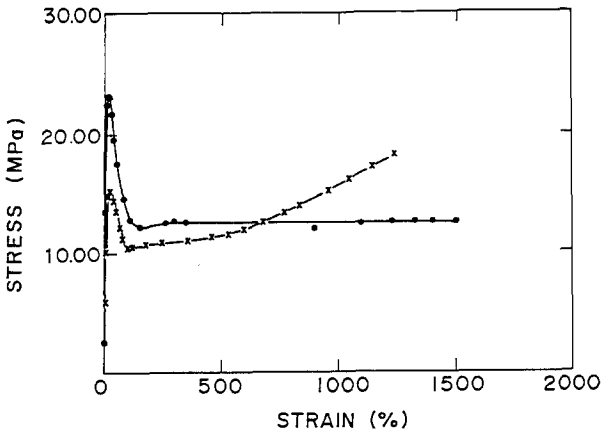

Figure 11 Stress–strain curves of (●) HPE and (x) CPE. $\dot{\varepsilon} = 0.4\,\text{min}^{-1}$, $T = 42°\,\text{C}$.

which the molecule must slide in order to disentangle, the slower the disentanglement rate. This is why ultra-high molecular weight PE has a high resistance to LSBF. The optimum molecular weight for resisting LSBF should be as large as possible, but there is a practical limitation. The difficulty of processing the material depends on the melt flow index which strongly depends on molecular weight. However, the density of short branches does not have a significant effect on the melt flow index.

The optimum length of the branch is an open question. For the critical application of gas piping the available commercial resins have branches that range from ethyl to hexyl. Bubeck and Baker's data [7] indicate that increasing the branch length increases the resistance to chain sliding. It is suggested that if the branch is longer than about eight carbon atoms, it will bend over as it slides through the crystal and will not be as resistant to sliding as a short stiff branch.

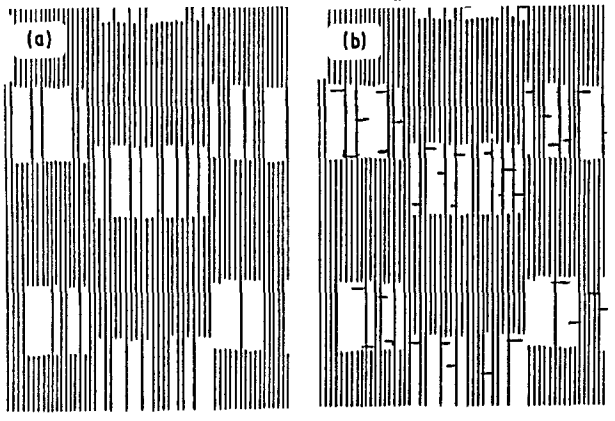

Figure 12 Schematic structures of highly oriented PE: (a) for HPE from paper by Gibson *et al.* [11] and (b) our modification for CPE. Light areas are amorphous regions.

Acknowledgements

The research was supported by the Department of Energy and the Gas Research Institute. The central facilities of the Materials Research Laboratory as supported by NSF were most helpful.

References

1. S. K. BHATTACHARYA and N. BROWN, *J. Mater. Sci.* **19** (1984) 2519.
2. *Idem, ibid.* **20** (1985) 2767.
3. *Idem, ibid.* **20** (1985) 4553.
4. X. LU and N. BROWN, *ibid.* **21** (1986) 2423.
5. *Idem, ibid.* **21** (1986) 4081.
6. M. K. V. CHEN and J. G. WILLIAMS, *Polymer* **24** (1983) 234.
7. R. A. BUBECK and H. M. BAKER, *ibid.* **23** (1982) 1680.
8. X. LU and N. BROWN, *ibid.* **28** (1987) 1505.
9. Y. HUANG, X. LU and N. BROWN, *Bull. Amer. Phys. Soc.* **32** (1987) 658.
10. N. BROWN, J. DONOFRIO and X. LU, *Polymer* **28** (1987) 1326.
11. A. G. GIBSON, S. A. JAWAD, G. R. DAVIES and I. M. WARD, *ibid.* **23** (1982) 349.

Received 24 April
and accepted 6 July 1987